Electron correlations in multiconfiguration atomic wave functions

David G. Ellis
Department of Physics and Astronomy, The University of Toledo, Toledo, Ohio 43606
(Received 23 January 1996)

A two-electron spin-independent operator is defined to represent the spatial correlation of the electrons in a general atom or ion. The spherical-tensor expansion of this operator provides a systematic method for evaluating the two-electron correlation function implied by a Hartree-Fock N-electron wave function including arbitrary configuration mixing. The method is illustrated by examples involving electron coalescence in helium and carbon, and core polarization in sodium. This technique for computing the electron correlation function provides a useful tool of wide applicability in comparing different theoretical approaches to the structure of complex atoms. [S1050-2947(96)06306-8]

PACS number(s): 31.10.+z, 31.25.−v

I. INTRODUCTION

A major challenge of atomic structure theory is to predict the correlation in the motion of the electrons in a complex atom. The most widely used computational techniques are based on the Hartree-Fock method with configuration interaction (HF CI); these calculations begin with the central-field approximation in which the electrons are uncorrelated. The influence of electron correlations is then accounted for indirectly, by using linear combinations of product wave functions. First Slater antisymmetrization, then Russell-Saunders coupling, and finally configuration mixing, allow for the correlations required by Fermi-Dirac statistics and by the noncentral character of the Coulomb interaction between electrons. Unfortunately the physical nature of the implied correlations is not necessarily obvious at the end of this process, from the resulting single-particle radial functions and configuration-mixing coefficients. This paper presents a method for analyzing the results of HF CI calculations so as to study directly the correlations of the electrons in space. This is a significant advance because it gives added insight into the physical nature of a multielectron quantum state, and because it allows detailed comparisons between wave functions resulting from different calculations.

In judging the expected precision of a result, or in comparing two different calculations, it would be useful to have a direct measure of the predicted correlation. In particular, a natural quantity to study would be the two-electron distribution function, $G_2(\vec{a},\vec{b})$, defined as the probability of finding an electron at point $\vec{a}$ and another at point $\vec{b}$. The purpose of this paper is to describe a general tensor-operator method for computing $G_2(\vec{a},\vec{b})$ from the results of a nonrelativistic many-configuration Hartree-Fock (MCHF) calculation in an atom or ion with N electrons. The nature of the predicted correlation can then be studied by means of G_2 and other functions easily calculated from it, such as the distribution in interelectron distances. After describing the computational method we first test it against previous work in helium and then apply it to certain states of the carbon and sodium atoms.

II. THEORY

A. Construction of the two-electron operator

We assume an atom or ion with N electrons described by the state function

$$|\Psi\rangle=\sum_{\gamma} C_{\gamma}|\Psi_{\gamma}(L,S,J,M)\rangle. \tag{1}$$

Each term in this expansion is a configuration state function (CSF) denoted by $|\Psi_{\gamma}(L,S,J,M)\rangle$ multiplied by a configuration-interaction coefficient C_{γ}. The CSF $|\Psi_{\gamma}\rangle$ is an LS-coupled antisymmetric basis state corresponding to the configuration $\gamma=\{(n_1l_1)^{w_1}(n_2l_2)^{w_2}\ldots\}$. In this configuration there are w_i electrons occupying the single-particle state (subshell) with quantum numbers (n_i,l_i) and radial wave function $\mathcal{P}_i(r)$.

The two-electron distribution function $G_2(\vec{a},\vec{b})$ is the expectation value of the corresponding operator $\hat{G}_2(\vec{a},\vec{b})$, which has an obvious form in the position representation:

$$\hat{G}_2(\vec{a},\vec{b})=\sum_{i=1}^{N}\sum_{j=1}^{i-1}[\delta^3(\vec{r}_i-\vec{a})\,\delta^3(\vec{r}_j-\vec{b}) + \delta^3(\vec{r}_i-\vec{b})\,\delta^3(\vec{r}_j-\vec{a})]. \tag{2}$$

The total integral gives twice the number of electron pairs: $\int G_2(\vec{a},\vec{b})d^3a\,d^3b=N(N-1)$.

If the atom is prepared in a pure quantum state $|\Psi\rangle$, then $G_2(\vec{a}\vec{b})=\langle\Psi|\hat{G}_2(\vec{a},\vec{b})|\Psi\rangle$ is a rather complicated function of six coordinates. However, three of the coordinates are just the Euler angles giving the orientation of the atom in space; these are irrelevant to our present purpose and we will average over them. Equivalently, since $\hat{G}_2(\vec{a},\vec{b})$ is spin independent, we can average over the directions of $\vec{L}$ and $\vec{S}$. In either case the result is a two-particle operator which depends only on the relevant variables a, b, and θ, the angle between $\vec{a}$ and $\vec{b}$:

$$\hat{G}(a,b,\theta)=\sum_{i<j}\left[\delta(r_i-a)\,\delta(r_j-b)+\delta(r_i-b)\,\delta(r_j-a)\right]\delta(\cos\theta_{ij}-\cos\theta). \quad (3)$$

Our two-particle distribution function is the expectation value of this operator, and is again normalized to twice the number of electron pairs:

$$G(a,b,\theta)=\langle\Psi|\hat{G}(a,b,\theta)|\Psi\rangle, \quad (4)$$

$$\int_0^\infty da\int_0^\infty db\int_{-1}^{+1}d\cos\theta\; G(a,b\,\theta)=N(N-1).$$

Defining $\hat{G}(a,b,\theta)$ in this way corresponds to using a spatially isotropic sample and selecting atoms by energy E_{LS} but not resolving the fine structure. Thus we neglect correlation effects caused by the spin-orbit interaction and by relativistic corrections, which we defer for future consideration.

B. Expansion in tensor operators

Since we want to be able to evaluate G using a general numerical CI wave function, it will be very convenient to express $\hat{G}$ in the language of spherical-tensor operators. Since $\hat{G}$ is a symmetric spin-independent two-electron operator, its behavior under rotations is identical to that of the Coulomb interaction operator $\hat{H}_C=\Sigma 1/r_{ij}$. Thus we can carry over the familiar analysis of $\hat{H}_C$ into a sum of Slater integrals multiplied by angular coefficients computed via Racah algebra. The first step is to introduce the standard partial wave expansion of $\hat{G}$:

$$\hat{G}(a,b,\theta)=\sum_{i<j}\sum_{k=0}^{\infty}G_{ij}^{(k)}(a,b,\theta)P_k(\cos\theta_{ij}), \quad (5)$$

$$G_{ij}^{(k)}(a,b,\theta)=\tfrac{1}{2}(2k+1)P_k(\cos\theta)\left[\delta(r_i-a)\,\delta(r_j-b)+\delta(r_i-b)\,\delta(r_j-a)\right].$$

Now we see that the standard Slater expansion of the matrix elements of $\hat{H}_C$ in terms of two-electron radial integrals can immediately be applied to our operator $\hat{G}$; the δ functions will convert the general Slater integral $R^k(i,j;i',j')$ into the direct and exchange radial functions (''Slater integrands''):

$$D^k_{\gamma\gamma'}(a,b,\theta)=\tfrac{1}{2}(2k+1)P_k(\cos\theta)\mathcal{P}_i(a)\mathcal{P}_j(b)\mathcal{P}_{i'}(a)\mathcal{P}_{j'}(b), \quad (6)$$

$$E^k_{\gamma\gamma'}(a,b,\theta)=\tfrac{1}{2}(2k+1)P_k(\cos\theta)\mathcal{P}_i(a)\mathcal{P}_j(b)\mathcal{P}_{i'}(b)\mathcal{P}_{j'}(a).$$

This leads to our principal result, valid for a general state of N electrons, where f_d^k and f_e^k are the standard direct and exchange Slater coefficients, which depend on γ,γ':

$$G(a,b,\theta)=\langle\Psi|\hat{G}|\Psi\rangle=\sum_k G_k(a,b)P_k(\cos\theta), \quad (7)$$

$$G_k(a,b)=\tfrac{1}{2}(2k+1)\sum_{\gamma\gamma'}C_\gamma C_{\gamma'}\mathcal{P}_i(a)\mathcal{P}_j(b)\left[f_d^k\mathcal{P}_{i'}(a)\mathcal{P}_{j'}(b)+f_e^k\mathcal{P}_{i'}(b)\mathcal{P}_{j'}(a)\right].$$

In this way it is straightforward to add the computation of $G(a,b,\theta)$ to any standard calculation based on the HF CI method. The required quantities are the mixing coefficients C_γ, the Slater coefficients f_d^k,f_e^k, and the radial functions $\mathcal{P}_i(r)$, all of which have already been computed during the HF CI calculation. In the present work we have done all calculations using the well-known MCHF-ASP program package of Froese Fischer [1], which provides these required quantities in the form of convenient data files.

C. Other spatial distribution functions

Having computed $G(a,b,\theta)$ as described above, we can gain some understanding of its nature by plotting the conditional probability density

$$P_C(a,\vec{r})=\frac{G(a,r,\theta)}{\rho(a)}. \quad (8)$$

This is the probability density for finding an electron at position $\vec{r}$ relative to the nucleus, given the condition that another electron is on the z axis, at distance a from the nucleus. Here $\rho(a)$ is the single-particle density, and the integrals of these functions satisfy

$$\int P_C(a,\vec{r})d^3r=N-1,\qquad \int\rho(a)d^3a=N. \quad (9)$$

Often more interesting is the difference between the P_C functions calculated with and without CI, which we designate $P_{\rm CI}$:

$$P_{\rm CI}(a,\vec{r})=P_C(a,\vec{r})_{\rm MCHF}-P_C(a,\vec{r})_{\rm HF}. \quad (10)$$

This function displays most directly the spatial correlation due to the noncentral part of the electron-electron interaction, the dynamic correlation distinct from that due to antisymmetrization and LS coupling. Sample plots of P_C and $P_{\rm CI}$ are given in Fig. 4.

Perhaps the most obvious diagnostic for electron correlation is the distribution in interelectron distances $F(s)$, known as the pair-distribution function (PDF). Define $F(s)ds$ as the number of electron pairs with separation $|\vec{a}-\vec{b}|$ having a value between s and $s+ds$. Using the coordinates [2] $p=a+b$, $q=a-b$, and $s=|\vec{a}-\vec{b}|$, we have

$$F(s)=\tfrac{1}{2}\pi^2 s\int_s^\infty dp\int_{-s}^{+s}dq(p^2-q^2)G_2(\vec{a},\vec{b}) \quad (11)$$

$$=s\int_s^\infty dp\int_{-s}^{+s}dq(p^2-q^2)^{-1}G(a,b,\theta). \quad (12)$$

Now $F(s)$ is normalized to count each pair only once:

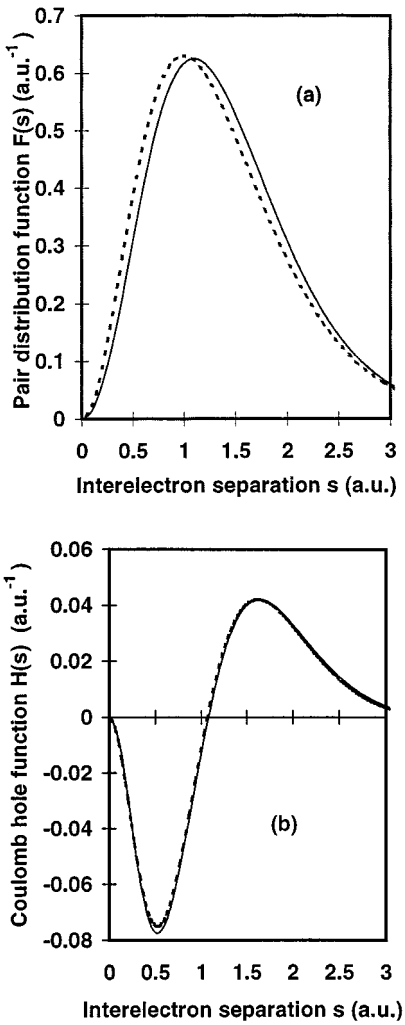

FIG. 1. The electron pair-distribution function (PDF) for the ground state of helium. (a) Solid curve: the correlated-variable result (RW) of Roothaan and Weiss [8], and the MCHF 20-configuration result, which are indistinguishable in this plot. Broken curve: the HF single-configuration result. (b) The Coulomb hole, that is, the PDF with the HF result subtracted; the difference between the two curves in (a). Solid curve, MCHF; broken curve, RW.

$$\int_0^\infty F(s)ds = \tfrac{1}{2}N(N-1). \tag{13}$$

From this function mean values such as $\langle s\rangle$ and $\langle 1/s\rangle$ can be calculated. Again we can subtract HF from CI results to study dynamic correlation: $H(s)=F_{\mathrm{MCHF}}(s)-F_{\mathrm{HF}}(s)$ has been called a *Coulomb hole* [3] *or correlation hole* [4] function by analogy with the *Fermi hole* which results from statistical correlation only.

As an alternative to $F(s)$ we can choose to study the pair-distribution volume density $R(s)=F(s)/4\pi s^2$, especially in the limit $s\to 0$. In some cases previous theoretical work, based on the symmetry of the wave function, has given interesting predictions about the volume density at a two-electron coalescence [5,6]. Examples of $F(s)$, $H(s)$ are plotted in Fig. 1, examples of $R(s)$ in Figs. 2 and 3.

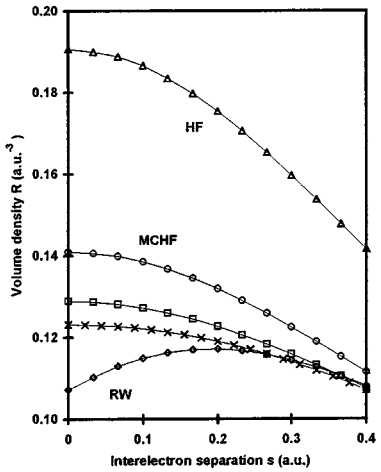

FIG. 2. The electron coalescence in the ground state of helium: the position probability density $R(s)$ for one electron at a distance s from the other. HF (triangles): Single-configuration Hartree-Fock; RW (diamonds): correlated-variables result of Roothaan and Weiss [8]; circles: MCHF AS2 (active set $n\leqslant 2$, 4 configurations); squares: MCHF AS3 (active set $n\leqslant 3$, 10 configurations); crosses: MCHF AS4 (active set $n\leqslant 4$, 20 configurations).

III. HELIUM TEST CASE

The $1s^2\,{}^1S$ ground state of neutral helium has been thoroughly studied using a variety of theoretical techniques, including calculations using correlated variables, which do not rely on the central-field approximation. We will not attempt to discuss the latest or most precise calculations, or the importance of relativistic corrections. Instead we are simply interested in testing the present method before applying it to more complex atoms. To that end we have computed MCHF

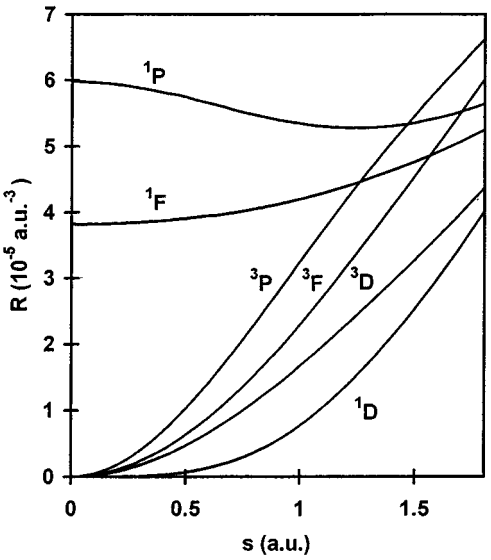

FIG. 3. Electron coalescence in the $2p3d$ states of carbon: the position probability density $R(s)$ for one electron at a distance s from the other. Note the different behavior of the natural-parity singlets (^1F,^1P), the triplets (^3F,^3D,^3P), and the unnatural-parity singlet ^1D. Calculations are single-configuration Hartree-Fock and only the $2p$,$3d$ electrons are included in the coalescence probability distribution.

TABLE I. Parameters describing pair-distribution function $F(s)$ for the helium ground state, computed from HF, MCHF, and Hylleraas wave functions.

	HF	MCHF (AS4)	Hylleraas [7]
$\langle s \rangle$	1.311	1.420	1.420
$\langle 1/s \rangle$	1.026	0.946	0.946
s at maxima	1.0	1.10	1.1
F(max)	0.632	0.625	0.625
$F(1.0)$	0.632	0.617	0.616
$F(2.0)$	0.274	0.308	0.311
$F(3.0)$	0.049	0.060	0.058

wave functions for the helium ground state using four different approximations, designated HF, AS2, AS3, and AS4, involving 1, 4, 10, and 20 configurations, respectively. The designation ASn refers to an ''active set'' calculation using all two-electron configurations which can be constructed from orbitals with principal quantum numbers 1–n. The functions $F(s)$, $H(s)$, and $R(s)$ computed from these solutions can now be compared with the corresponding functions resulting from calculations using correlated variables.

Coulson and Neilson [7] have computed the pair-distribution and Coulomb hole functions which result from the pioneering correlated-variables calculation of Hylleraas [2]. Our results using the AS4 basis are virtually identical with theirs, as shown in Table I; also shown for comparison are the single-configuration Hartree-Fock results.

A more elaborate correlated-variables result, which is convenient for the present purpose, is that of Roothaan and Weiss [8]. Their ''correlated open-shell'' wave function has 20 adjustable parameters, and accounts for 99% of the correlation energy computed in the definitive work of Pekeris [9]. Figures 1 and 2 compare our MCHF results for the functions $F(s)$, $H(s)$, and $R(s)$ with the corresponding functions computed from the wave function of Roothaan and Weiss (RW). These comparisons verify that our tensor-operator method is giving the correct functions. They also serve to highlight the degree to which a relatively simple MCHF wave function can approach a fully correlated result. In particular, Fig. 2 shows the situation with electron coalescence by plotting the pair separation probability density $R(s)$. The HF calculation seriously overestimates $R(s)$ for small s, but MCHF dramatically improves the agreement with RW by adding only a few configurations. Note, however, that the RW result satisfies the Kato [6] cusp condition $R'(0)=R(0)$, while the MCHF results do not because of the limitations of the global basis on which they are constructed.

IV. SAMPLE APPLICATIONS

A. Electron coalescence in the $2p3d$ states of carbon

It is well known that Fermi-Dirac statistics and spin-orbit coupling conditions combine to place restrictions on the behavior of two-electron wave functions in the vicinity of a coalescence. Kutzelnigg and Morgan [10] have analyzed these restrictions for a configuration of type $n_1l_1n_2l_2$, with $l_1,l_2>0$, and in particular for the configuration $2p3d$ in neutral carbon [5]. They find there are three classes of LS-coupled terms, with regard to the behavior of the wave function as the electron separation approaches zero. For the natural-parity singlets, $R(0)$ is finite; for the triplets, $R(s)$ has a quadratic zero at $s=0$; for the unnatural-parity singlets, a quartic zero.

This behavior can be displayed quantitatively by using our tensor expansion method to compute $R(s)$ for the carbon configuration $2p3d$. Figure 3 shows the results for $R(s)$ near $s=0$ produced by doing an LS-dependent HF calculation [1] for each of the six terms separately, and computing the pair-distribution function for just the two outer electrons. The separation of the unnatural-parity ^1D from the other terms is clear. Note, however, that if all six (or the four outer) electrons are included in the computation of the PDF, the results shown in Fig. 3 will be obscured by the larger values of $R(0)$ associated with the $1s$ and $2s$ orbitals (core correlations).

B. Core polarization in sodium

In discussing the sodium $3s$-$3p$ line strength, Brage, Froese Fischer, and Jönsson [11] have stressed the distinction between core-valence (CV) and core-core (CC) correlations, and the importance of including both. Using our tensor-operator method, we can readily illustrate the difference in the core polarization associated with these two types of correlation by plotting the conditional probability distribution $P_c(a,\vec{r})$ for the Na I $3p$ state. For this purpose it is sufficient to consider the seven-electron system $2p^63p\,^2P$ with an inert four-electron core $1s^22s^2\,^1S$. For this $N=7$ system we compute $P_C(a,\vec{r})$ with one electron fixed near the maximum in the $3p$ radial distribution.

We have done four relatively simple MCHF [1] calculations of this state, which we identify as HF, CV, CC, and CVC. HF is a single-configuration Hartree-Fock calculation for $2p^63p\,^2P$. CV includes all configurations of type $2p^5nln'l'\,^2P$, with $n,n'\leqslant 4$, resulting in 44 CSFs. CC includes all configurations of type $2p^43pnln'l'\,^2P$, with $n,n'\leqslant 4$, resulting in 260 CSFs. CVC uses all configurations of both types, and results in 303 CSFs. The $n=1,2$ orbitals were determined by HF, and then held fixed during the other calculations. Calculations CV and CC were independent MCHF calculations, with the seven outer orbitals ($n=3,4$) being determined self-consistently in each case. Finally, in calculation CVC no orbitals were varied; instead, a CI calculation was done, with the $1s,2s,2p$ radial functions having been determined by HF, the $3s,3p,3d$ functions by CC, and the $4s,4p,4d,4f$ functions by CV. Thus CVC is intended to show a combination of the core-valence and core-core types of correlation. The two-electron correlations predicted by these four calculations are shown in Figs. 4 and 5.

Figure 4(a) shows the result for $P_C(a,\vec{r})$ given by the HF (single-configuration) solution. Here we are assuming one electron is on the z axis at $a=5.0$ a.u., and plotting the probability distribution of the remaining six electrons as a

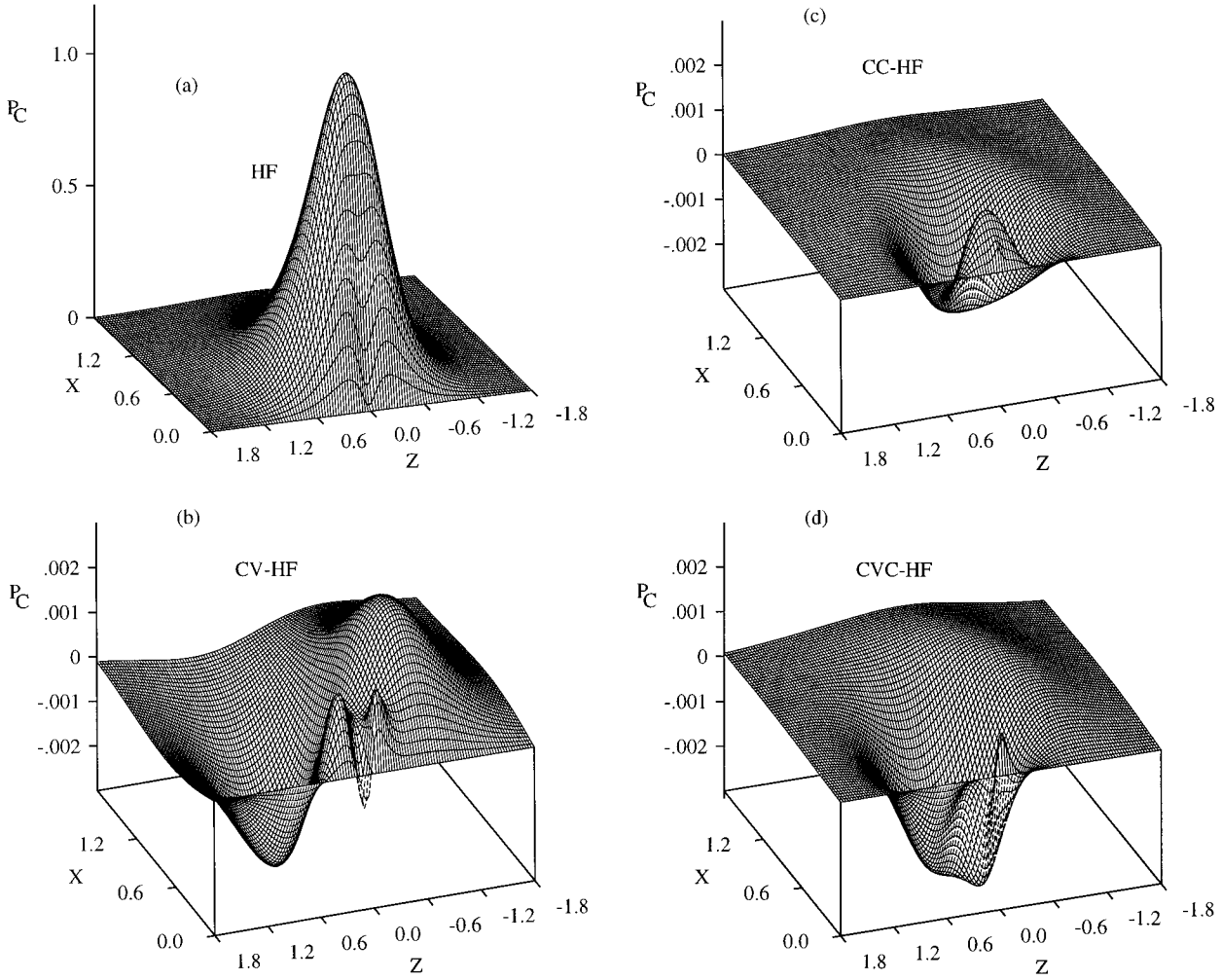

FIG. 4. Core polarization in the $3p$ state of sodium: the conditional probability $P_C(a,\vec{r})$ for an electron at $\vec{r}$ given an electron on the $+z$ axis at $z=5$ a.u. Only the seven electrons outside a frozen $1s^2 2s^2$ core are considered. The quantity plotted on the vertical axis is $2\pi x P_C$; the integral over the xz half plane with $x>0$ gives $N-1=6$. The units for the horizontal axes are a.u., for the vertical axis a.u.$^{-2}$. The calculations HF, CV, CC, CVC are described in the text; CV contains core-valence correlation only, while CC contain core-core correlation only. (a) the Hartree-Fock result; (b) the difference CV$-$HF; (c) the difference CC$-$HF; (d) the difference CVC$-$HF which shows the combined effect.

function of $\vec{r}$. Since $P_C(a,\vec{r})$ is symmetric under rotations about the z axis, the functions plotted in Fig. 4 have been multiplied by $2\pi x$ for normalization per unit area in the xz plane, with $x=r\sin\theta$, so that

$$\int_0^\infty dx \int_{-\infty}^{\infty} dz[2\pi x P_C(a,\vec{r})]=6. \tag{14}$$

The plots of $P_C(a,\vec{r})$ for all four solutions look very similar, since the configuration mixing for this case is small: the leading CI coefficient is at least 0.99 in each solution. Nevertheless, interesting and reproducible patterns emerge if we plot the difference functions $P_{\mathrm{CI}}(a,\vec{r})$, which reflect the correlation due to configuration mixing. These plots are shown in Fig. 4(b) for calculation CV, Fig. 4(c) for CC, and Fig. 4(d) for CVC.

Calculation CV gives the expected result that the $2p^6$ core electron distribution is distorted by the presence of the outer electron on the $+z$ axis, with the charge density being displaced in the $-z$ direction relative to HF, as shown in Fig. 4(b). On the other hand, calculation CC, shown in Fig. 4(c), does not give a dipole polarization, although it is a bigger calculation and results in a lower energy. The symmetry of the CC result is also expected, since the core-core correlations included tend to maintain the physical picture of a single $3p$ electron outside a spherical six-electron core. However, this symmetry is not exact; it is dependent on the fact that we chose to compute $P_{\mathrm{CI}}(a,\vec{r})$ with a chosen at a distance characteristic of the $3p$ orbital, and well outside the $2p^6$ core. If the first electron is placed closer to the nucleus, then the other six are not distributed symmetrically. Calculation CVC, containing all the configurations of both CV and CC, gives the pattern of core polarization shown in Fig. 4(d).

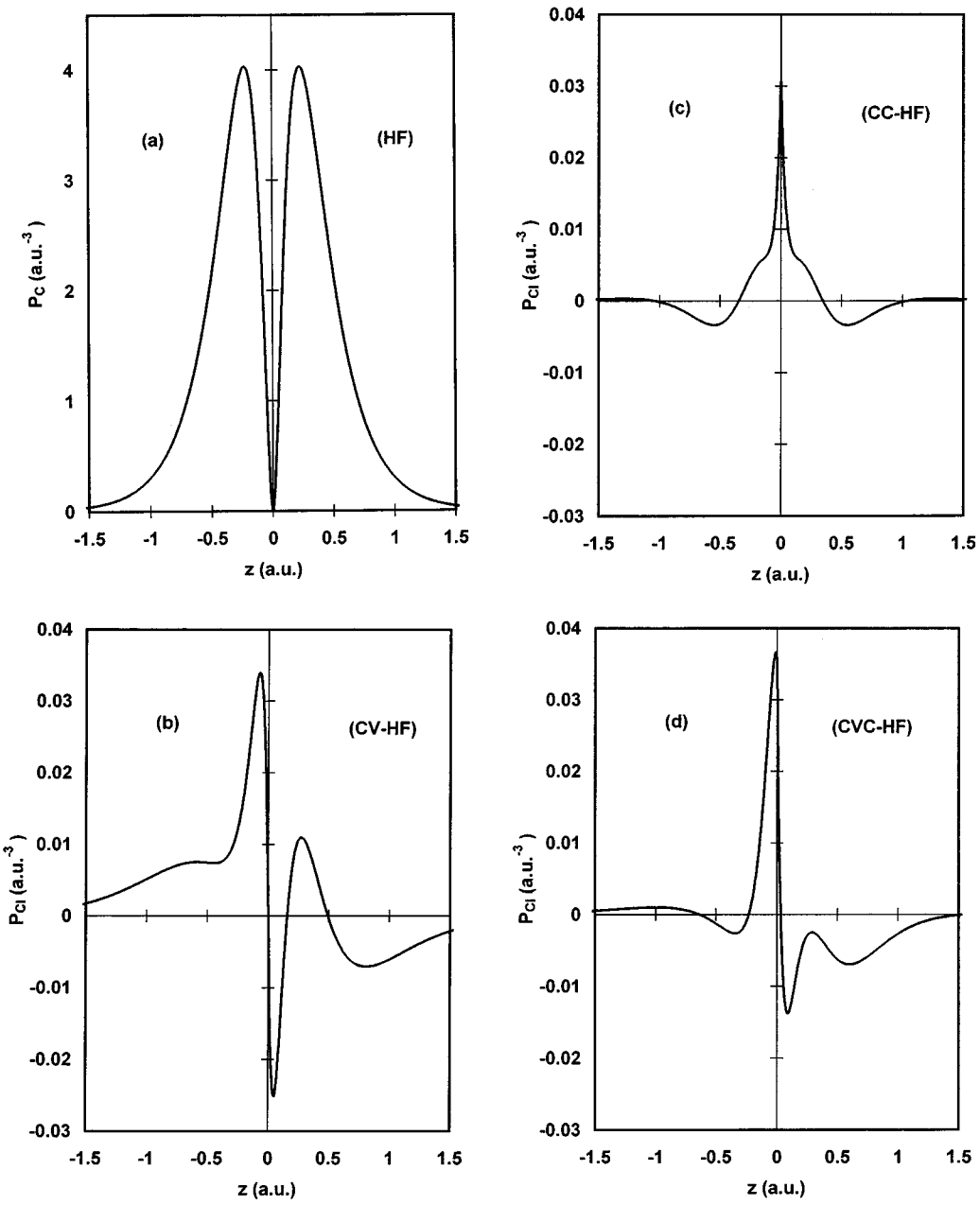

FIG. 5. Core polarization in the $3p$ state of sodium: with one electron on the $+z$ axis at $z=5$ a.u., the probability density of the other six electrons along the z axis. (a) The Hartree-Fock result; (b) the difference CV−HF; (c) the difference CC−HF; (d) the difference CVC−HF.

Clearly this has a strong dipole component, but is quite different in detail from the polarization predicted by core-valence interactions alone.

Plots such as those in Fig. 4 give a valuable global view of the correlation functions P_C and P_{CI}; however, we can obtain more detailed information by making cuts in various directions through these distributions. Figure 5 shows plots of $P_C(a,\vec{r})$ and $P_{\mathrm{CI}}(a,\vec{r})$ as a function of z for fixed $x=0$ and $a=5.0$ a.u. In other words, this is the volume density of core electrons along the line joining the outer electron and the nucleus; Fig. 5(a) shows the HF result. As with the plots in Fig. 4 it must be emphasized that we are considering only seven electrons. If the four electrons in the frozen $1s^2 2s^2$ core were included, they would produce a sharp peak near the nucleus instead of the dip in Fig. 5(a), which is caused by the zero in the $2p$ radial function at $r=0$. Again Figs. 5(b), 5(c), and 5(d) show the CV, CC, and CVC results, respectively, with the HF result subtracted.

Finally, we consider the core-core correlations further by using the CC wave function to compute $P_{\mathrm{CI}}(a,\vec{r})$ for several values of a. Figure 6 shows plots of these results with $\vec{r}$ on the z axis, as in Fig. 5. The symmetry of Figs. 4(c) and 5(c) is now lost as we consider the correlation between electron pairs closer to the nucleus. In Fig. 6 the position of one electron is indicated by the dot on the $+z$ axis in each case. For an exact solution, P_C, and therefore also P_{CI}, must have a zero or a cusp at that coalescence point [6]. As in the case

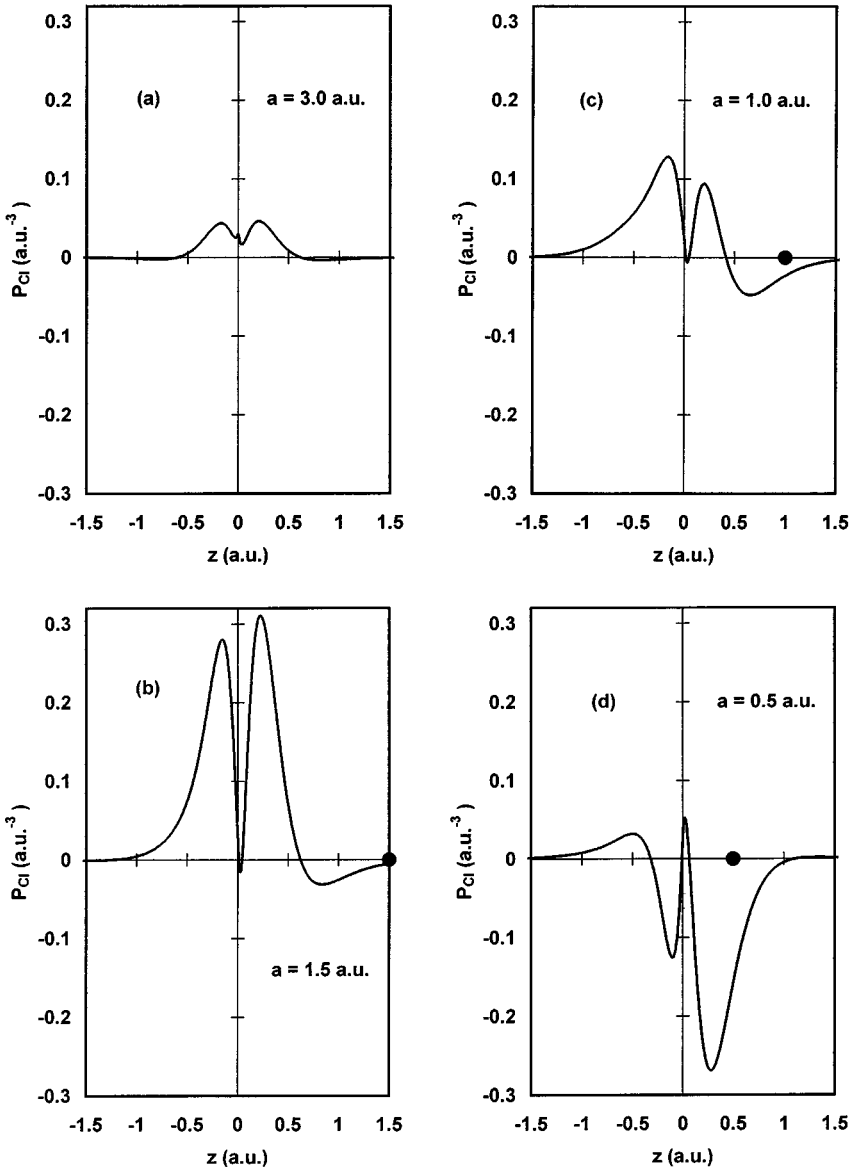

FIG. 6. Core correlation in the $3p$ state of sodium: $P_{\mathrm{CI}}(a,\vec{r})$ for $\vec{r}$ on the z axis, with various values of a, using the results of calculation CC (260 CSFs). (a) $a=3.0$ a.u.; (b) $a=1.5$ a.u.; (c) $a=1.0$ a.u.; (d) $a=0.5$ a.u.

of helium (Fig. 2) we note the necessary absence of such cusps in the MCHF results.

V. CONCLUSION

The tensor expansion shown in Eq. (7) provides a general method for computing the two-electron spatial correlation function $G(a,b,\theta)$, the probability of finding electrons at both points $\vec{a}$ and $\vec{b}$. This method can be applied to the results of any HF CI calculation which provides a wave function specified by single-particle radial functions and configuration-mixing coefficients.

The two-electron correlation function provides fresh insight into the nature of HF CI solutions; it gives an additional point of comparison between different calculations, which is especially useful in cases where experimental data are lacking. In the future this method could provide a helpful connection between theoretical descriptions of atomic structure based on the central-field approximation and those using other methods, including correlated variables.

Finally we note that this tensor-operator formalism can be extended in a straightforward way to apply to Dirac wave functions. A program is now being developed to compare directly the correlations predicted by MCHF [1] and multiconfiguration Dirac-Fock (MCDF) [12] calculations. Such comparisons should be helpful in studying the relative effectiveness of these two approaches for various classes of problems.

ACKNOWLEDGMENTS

It is a pleasure to acknowledge valuable interactions with Tomas Brage, Robert Cowan, Larry Curtis, Alan Hibbert, Constantine Theodosiou, and especially Charlotte Froese Fischer. Some calculations were supported by Grant No. PJS216-1 from the Ohio Supercomputer Center. Help with the computation and graphics was provided by Jens Petersohn and Rasa Matulioniene of The University of Toledo, and by Todd Leonhardt, who was supported by Grant No. PHY-9200403 from the National Science Foundation. Many personal thanks are due for the encouragement and support of Indrek Martinson and the hospitality of the Physics Department at The University of Lund.

[1] C. Froese Fischer, Comput. Phys. Commun. **64**, 369 (1991).
[2] E. A. Hylleraas, Z. Phys. **54**, 347 (1929); Adv. Quantum Chem. **1**, 1 (1964).
[3] R. Benesch and V. H. Smith, Jr., J. Chem. Phys. **55**, 482 (1971).
[4] N. H. March, *Self-Consistent Fields in Atoms* (Pergamon, New York, 1975).
[5] J. D. Morgan III and W. Kutzelnigg, J. Phys. Chem. **97**, 2425 (1993).
[6] T. Kato, Commun. Pure Appl. Math. **10**, 151 (1955).
[7] C. A. Coulson and A. H. Neilson, Proc. Phys. Soc. London **78**, 831 (1961).
[8] C. C. J. Roothaan and A. W. Weiss, Rev. Mod. Phys. **32**, 194 (1960).
[9] C. L. Pekeris, Phys. Rev. **126**, 1470 (1962).
[10] W. Kutzelnigg and J. D. Morgan III, J. Chem. Phys. **96**, 4484 (1992).
[11] T. Brage, C. Froese Fischer, and P. Jönsson, Phys. Rev. A **49**, 2181 (1994).
[12] K. G. Dyall, I. P. Grant, C. T. Johnson, F. A. Parpia, and E. P. Plummer, Comput. Phys. Commun. **55**, 425 (1989).